



Published in final edited form as:

*Cytotherapy*. 2020 May ; 22(5): 291–300. doi:10.1016/j.jcyt.2020.01.013.

## Understanding the freezing responses of T-cells and other subsets of human peripheral blood mononuclear cells using DMSO-free cryoprotectants

Chia-Hsing Pi<sup>1,\*,\*\*</sup>, Kathlyn Hornberger<sup>2,\*\*</sup>, Peter Dosa<sup>3</sup>, Allison Hubel<sup>1,2,\*</sup>

<sup>1</sup>Department of Mechanical Engineering, University of Minnesota, Minneapolis, 55455, USA

<sup>2</sup>Department of Biomedical Engineering, University of Minnesota, Minneapolis, 55455, USA

<sup>3</sup>Institute for Therapeutics Discovery and Development, University of Minnesota, Minneapolis, 55455, USA

### Abstract

This study examined the freezing responses of peripheral blood mononuclear cells (PBMCs) and specific white blood cell subsets contained therein when cryopreserved in three combinations of osmolytes composed of sugars, sugar alcohols and amino acids. A differential evolution algorithm with multiple objectives was used to optimize cryoprotectant composition in order to optimize the post-thaw recoveries for both helper and cytotoxicity T-cells simultaneously. The screening of various formulations using differential evolution algorithm showed post-thaw recoveries over 80% for the two subsets of T-cells. The phenotypes and viabilities of PBMC subsets were characterized using flow cytometry. Significant differences between the post-thaw recovery for helper T-cell and cytotoxic T-cell were observed. Statistical models were used to analyze the importance of individual osmolytes and interactions between post-thaw recoveries of three subsets of T-cell including helper T-cells, cytotoxic T-cells and natural killer T-cells. The statistical model indicated that the preferred concentration levels of osmolytes and interaction modes were distinct between these three subsets studied. PBMCs were cultured for 72 hours post-thaw to determine the stability of the cells. As post-thaw apoptosis is a significant concern for lymphocytes, apoptosis of helper T-cell and cytotoxic T-cells frozen in a DMSO-free cryoprotectant was analyzed immediately post-thaw and 24 hours post-thaw. Both cell types showed a decrease in cell viability 24 hours post-thaw compared to immediately post-thaw. Helper T-cell viability dropped 17%, and cytotoxic T-cells had a 10% drop in viability. Immediately post-thaw, both cell types had >30% of cells in early apoptosis, but after 24 hours the number of cells in early apoptosis decreased to below 20%.

\*Corresponding author: Allison Hubel, PhD: University of Minnesota, 111 Church St. SE, Minneapolis, MN 55455. Phone: 612-626-445. Fax: 612-625-4344. hubel001@umn.edu.

\*\*These two authors contributed equally to the work.

#### Author contributions

C.-H. P. designed research, performed experiments, analyzed data, and wrote the manuscript. K. H. designed research, performed experiments, analyzed data, and wrote the manuscript. P.D. and A. H. designed research and wrote the manuscript.

#### Competing interests

The authors declare no competing interests.

**Publisher's Disclaimer:** This is a PDF file of an unedited manuscript that has been accepted for publication. As a service to our customers we are providing this early version of the manuscript. The manuscript will undergo copyediting, typesetting, and review of the resulting proof before it is published in its final form. Please note that during the production process errors may be discovered which could affect the content, and all legal disclaimers that apply to the journal pertain.

This study helped us to identify the freezing responses of different human PBMC subsets using combinations of osmolytes.

## Keywords

peripheral blood mononuclear cell; cryopreservation; DMSO-free cryoprotectant; T-cells

---

## Introduction

Immunotherapies such as chimeric antigen receptor (CAR) T-cell therapy are emerging therapies for the treatment of cancers and persistent viral infections [1,2]. Human peripheral blood mononuclear cells (PBMCs), which are typically harvested using apheresis, is the starting material for most immunotherapies. It is common for apheresis products to be collected in one location and processed in another location. The PBMCs must remain viable along this supply chain; therefore, an effective method of cryopreserving PBMCs is critical for clinical use.

Dimethyl sulfoxide (DMSO) has been the gold standard in cryopreservation for over half a century [3] for both research and clinical applications [4–10]. However, DMSO is toxic to PBMCs [11,12], resulting in cell losses as a function of time of exposure. In addition, significant adverse events have been reported in patients resulting from the administration of cells containing DMSO [4,8,10,13–16]. As a result, there is an urgent demand for finding improved methods of cryopreserving cells that use non-toxic alternatives to DMSO [4,7].

Previous studies of the cryopreservation of PBMCs [7,9,10,13,14,17,18] treated PBMCs as a homogeneous population. However, PBMCs are a heterogeneous population comprised of multiple cell types, including lymphocytes such as B cells, T-cells, and NK cells, and monocytes [19]. Neglecting the differential responses of the various cell types that make up PBMCs can lead to suboptimal outcomes. Certain subsets may be depleted during cryopreservation, which may be hidden if overall recovery is determined.

In our previous work [20–25], we optimized DMSO-free cryoprotectants for Jurkat cells using mixtures of sugars, sugar alcohols and amino acids. These natural osmolytes act by stabilizing biological systems subjected to environmental extremes [26]. Using the Jurkat immortalized lymphocyte cell line allowed for high-throughput screening of cryoprotectant solutions. Additionally, mechanisms of action and interactions between osmolytes have been previously characterized using Raman spectroscopy and statistical modeling [20,21]. Raman images showed the influence of osmolytes on ice crystal shape, which reflects the interactions between osmolytes and water. Both higher concentrations of glycerol and interactions between sugars and glycerol were found to increase the post-thaw recovery. Jurkat cells were used for screening osmolyte solution compositions [20,21] and the optimal compositions for each formulation were then used in this study to cryopreserve PBMCs. The post-thaw recoveries of Jurkat cells cryopreserved with optimal formulations of SGI (Sucrose-Glycerol-Isoleucine), TGI (Trehalose-Glycerol-Isoleucine), and MGI (Maltose-Glycerol-Isoleucine) were 84%, 84%, and 85%, respectively [20,21].

In this work, we conduct a comparative study to evaluate the effects of three DMSO-free cryoprotectants optimized for Jurkat cells on human PBMC subsets. The evaluations include the post-thaw recovery of T-cells (CD3+CD56<sup>-</sup>), as well as T-cell subsets including helper T-cell (CD3+CD4<sup>+</sup>) and cytotoxic T-cell (CD3+CD8<sup>+</sup>). This work provides critical insight into the potential of DMSO-free cryoprotectants in terms of preserving a heterogeneous population and analyzing the freezing response of each subpopulation in osmolyte-based cryoprotectants.

## Methods and Backgrounds

### PBMC collection and study participants

Samples were collected from healthy volunteers (n=10 including 3 females and 7 males, age: 39–70, mean age: 55.7 and median: 57.5), with informed consent and IRB approval at Memorial Blood Center (Saint Paul, MN). Peripheral blood mononuclear cells (PBMCs) were recovered from leukoreduction system chambers (LSCs, Terumo BCT, Lakewood, CO, USA) [27]. PBMCs were stored overnight at room temperature and atmospheric conditions. There was no significant difference between male and female donors in terms of the composition of PBMCs pre-freeze.

### Jurkat cell culture

Jurkat cells (ATCC TIB-152) were used in this work as a model CD3<sup>+</sup> T-cell. The cell line identification was done by Short Tandem Repeat (STR) through the American Type Culture Collection. Cells were cultured in a combination of high-glucose RPMI1640 (Life Technologies, Carlsbad, CA, USA) and 10% fetal bovine serum (FBS; Qualified, Life Technologies, Carlsbad, CA, USA). The cell concentration in culture was maintained between  $1 \times 10^5$  and  $3 \times 10^6$  cells/mL.

### Cryoprotectants

Our previous work has shown that multicomponent osmolyte solutions including sugars, sugar alcohols and amino acids are effective in cryopreserving cells [20,21,24]. Three osmolyte-based and DMSO-free cryoprotectant combinations, sucrose-glycerol-isoleucine (SGI), trehalose-glycerol-isoleucine (TGI), and maltose-glycerol-isoleucine (MGI), were used in this work. The concentration space of each osmolyte was discretized to six levels with equal space, the highest level is set up by either toxicity limits or solubility limits. The concentration levels as well as the optimal formulation have been published previously [20]. There were 216 possible formulations for each combination of osmolytes. All DMSO-free cryoprotectants were prepared in Normosol-R (Hospira, Lake Forest, IL, USA). A 10% DMSO solution in Normosol-R was used as control.

### Plate freezing and post-thaw assessment

Both Jurkat cells and PBMCs were cryopreserved in clear-bottom black 96-well plates (Corning, NY, USA) for high-throughput screening of DMSO-free cryoprotectants. Previous studies [23] demonstrated that the outer layer of wells exhibited different freezing and thawing behavior from the inner. As a result, only column 2–11 and row B–G (60 wells in total) contained cells and solutions. Solutions of interest were made at 2 $\times$  of final

concentration in Normosol-R. Samples were centrifuged at  $125\times g$  for 10 min and resuspended in Normosol-R and then combined 1:1 with test solutions to produce a  $1\times$  concentration of test solution with 300,000 cells/well in  $50\mu\text{L}$  (6 million cells/mL). Samples were also cryopreserved in 10% DMSO in Normosol-R as a control. All studies were performed in triplicate wells on each plate. The cells were incubated in the solutions of interest for one hour at room temperature under atmospheric conditions prior to freezing.

A controlled rate freezer (Kryo 560; Planer, Middlesex, UK) was used to cryopreserve all samples. Microplates were placed in a rack, and frozen using the following cooling curve: (1) start at  $20^{\circ}\text{C}$ , (2)  $-10^{\circ}\text{C}/\text{min}$  to  $0^{\circ}\text{C}$ , (3) hold at  $0^{\circ}\text{C}$  for 15 min, (4)  $-1^{\circ}\text{C}/\text{min}$  to  $-8^{\circ}\text{C}$ , (5)  $-50^{\circ}\text{C}/\text{min}$  to  $-45^{\circ}\text{C}$ , (6)  $+15^{\circ}\text{C}/\text{min}$  to  $-12^{\circ}\text{C}$ , (7)  $-1^{\circ}\text{C}/\text{min}$  to  $-60^{\circ}\text{C}$ , and (8)  $-10^{\circ}\text{C}/\text{min}$  to  $-100^{\circ}\text{C}$ . The rapid cooling and rewarming (steps 5 and 6) were used to induce nucleation in the extracellular solution. After the freezing procedure was completed, plates were stored on vapor-phase liquid nitrogen for a minimum of 24 hours up to several days until thawed.

Thawing was performed in a  $37^{\circ}\text{C}$  water bath, and thawing was complete in less than 3 mins. Calcein acetoxymethyl (Calcein-AM, Life Technologies) and propidium iodine (PI, Life Technologies) in Phosphate-Buffered Saline (PBS) were used to determine post-thaw cell recovery. Calcein-AM/PI dye was added to each well at a 1:1 ratio between tested solution and dye. After the addition of dye, the plates were wrapped in aluminum foil and incubated for 30 min at  $37^{\circ}\text{C}$  and 5%  $\text{CO}_2$ . The fluorescence of each plate was read at 530/590 nm and 485/528 nm for PI and Calcein-AM, respectively (Synergy<sup>TM</sup> HT, BioTek Instruments, Winooski, VT, USA). The bandwidths were 530/25 and 590/35 for PI and 485/20 and 528/20 for Calcein-AM for excitation and emission, respectively.

All fluorescent intensities of PBMC and Jurkat cryopreserved in DMSO-free cryoprotectants were normalized by the fluorescent intensities of DMSO-containing cryoprotectant for comparison purposes.

### Vial Freezing and Thawing

Vial-freezing experiments were performed in order to understand the freezing responses of PBMC subpopulations using larger volumes. PBMCs were diluted with Normosol-R (Hospira, IL, USA), and then cell suspensions were transferred into cryovials and then combined 1:1 with  $2\times$  cryoprotectants to make a final volume of 1 mL with cell concentration between  $5\times 10^6$  and  $25\times 10^6$  cells/mL. Cell suspensions were cryopreserved in 10% DMSO in Normosol-R as a control. Vials were cryopreserved under the same cooling profile as plate freezing. After the freezing procedure, vials were transferred to vapor-phase liquid nitrogen for a minimum of 24 hours before thawing. Thawing was performed in a  $37^{\circ}\text{C}$  water bath, and thawing was complete in less than 3 mins. The proportion of each subset and the viability of thawed vials were characterized by flow cytometry.

### Flow Cytometric Characterization of Phenotype and Viability

Freshly isolated and thawed PBMC were used for flow cytometry to analyze the proportion and viability of each population. For each PBMC sample, phenotype staining was done before freezing (fresh) and immediately after thawing in order to calculate the post-thaw

recoveries. The cell concentration of white blood cells (CD45+) was measured with the Z1 Particle Counter (Beckman Coulter, Brea, CA). Nine panels of antibodies were used to determine the proportions of PBMC subsets and their viabilities. The information for fluorophores, antibodies, and manufacturers is shown in Table 1. The gating strategy of all PBMC subsets was determined by first identifying all white blood cells (CD45+). From this plot, granulocytes (CD15+), monocytes (CD14+), and lymphocytes (CD14-CD15-) were identified. From the lymphocyte plot, B cells (CD19+), NK cells (CD3-CD56+), NKT cells (CD3+CD56+), and T-cells (CD3+CD56-) were determined. Finally, from the T-cell subset, helper T-cells (CD3+CD4+) and cytotoxic T-cells (CD3+CD8+) were identified. The full gating strategy is shown in Figure 1. The data was collected with a BD LSR II (BD Bioscience, San Jose, CA) flow cytometry with FACSDiva software (version 8.0.1), and the data analysis was performed using FlowJo 9.8.5 software (Tree Star, Ashland, OR) according to established protocols.

The staining protocol is briefly described as following. Antibody cocktails were added to PBMC samples and incubated for 30 mins at 4°C under a low light environment. BD FACS Lysing 10x solution (BD Biosciences, San Jose, CA) was added and cells were incubated for 15 mins at room temperature. Cells were centrifuged for 5 min at 500×g, the supernatant was removed, and a staining buffer was added (BD Pharmingen, San Jose, CA). Samples were recentrifuged for 5 min at 500×g, the supernatant was removed and fixation buffer was added. Samples were stored at 4°C under a low light environment until acquisition.

The post-thaw recovery was calculated according to Equation 1.

$$\text{post - thaw recovery} = \frac{\text{number of viable cells post - thaw}}{\text{number of viable cells pre - freeze}} \times 100\% \quad (1)$$

### Flow Cytometric Characterization of Post-thaw Apoptosis

Post thaw apoptosis was determined using PBMCs frozen in TGI cryoprotectant. Cells were thawed rapidly in a water bath for 2 minutes and 30 seconds and then stained for caspases per manufacturer's instructions (Vybrant FAM poly caspases assay kit, Life Technologies, Carlsbad, CA). Cells were incubated with FLICA reagent for 60 minutes at 37°C and 5% CO<sub>2</sub> in the dark. Cells were washed twice with apoptosis wash buffer, stained for CD4 and CD8, and incubated in the dark at room temperature for 15 minutes. After a final wash step, cells were stained with a viability dye (ViaProbe, 7-AAD, BD Biosciences). Information for each antibody is included in Table 2.

Fractions of viable, early and late apoptotic, and necrotic CD4+ and CD8+ T-cells were determined. Viable cells stained negative for both caspases and 7-AAD. Cells in early apoptosis stained positive for caspases and negative for 7-AAD, while cells in late apoptosis stained positive for caspases and 7-AAD. Necrotic cells stained negative for caspases, but positive for 7-AAD.

The gating strategy identified lymphocytes from forward scattering channel (FSC) and side scattering channel (SSC). A gate was applied to FSC-W and FSC-H to select only single T-

cells. CD4<sup>+</sup> and CD8<sup>+</sup> cells were identified, which indicate helper T-cells and cytotoxic T-cells, respectively. An apoptosis vs 7-AAD plot was created for each cell type.

### Differential evolution algorithm

Optimization of the cryopreservation solution composition was performed using the differential evolution (DE) algorithm developed by Storn and Price [28] as shown in Figure 2. This approach utilizes stochastic direct search and independent perturbation of population vectors to localize the global maximum within the entire parameter space. The algorithm was performed using Python version 3.7.0 (Python Software Foundation, 2019). In the optimization process, eight different formulations were generated randomly through the parameter space. The post-thaw recoveries of both helper T-cell and cytotoxic-T-cell for the different formulations tested were given to the algorithm, and then the algorithm generated a new set of formulations for testing. When the post-thaw recoveries of each subset were distributed in a range within 20% (i.e.  $\pm 10\%$ ) variation, this situation was defined as convergence.

A conventional DE algorithm was used to screen freezing responses of PBMC under various formulations of DMSO-free cryoprotectants. In order to optimize the post-thaw recoveries of multiple subsets simultaneously, a specific variant of differential evolution for multiple objectives (DEMO) was customized based on the development by Robi et al. [29]. The DEMO algorithm only differs from the original DE algorithm by selecting new formulations to test based on the post-thaw recovery of two subsets of cells. The DE algorithm consists of 27 lines of code that is available as open source software at <http://www.icsi.berkeley.edu/~storn>. More details on the application of this algorithm can be found in [23,30].

### Post-thaw culture of PBMCs

Thawed PBMCs were washed and centrifuged twice in Normosol-R at 125 $\times$ g for 10 min and then cultured in high-glucose RPMI 1640 with 10% fetal bovine serum. The initial density was maintained at  $1 \times 10^6$  cells/mL. The viability and cellular density were measured at 0, 24, 48, 72 hours post-thaw.

### Differential scanning calorimetry

Differential scanning calorimetry (DSC) was performed on a TA Differential Scanning Calorimeter Q1000 (TA Instruments, Eden Prairie, MN, USA). Cryoprotectants without cells were loaded into T zero pans and hermetically sealed. Samples were frozen to  $-150^\circ\text{C}$  using the following protocol: (1) start at  $20^\circ\text{C}$ , (2) cool to  $-150^\circ\text{C}$  at  $10^\circ\text{C}/\text{min}$ , (3) hold for 3 min at  $-150^\circ\text{C}$ , and (4) warm to  $20^\circ\text{C}$  at  $10^\circ\text{C}/\text{min}$ . DSC results were analyzed using TA Universal Analysis version 4.5A.

### Statistical Analysis

Statistical modeling was performed using R version 3.4.0 (R Core Team, 2019) for Windows OS. The variation in post-thaw recovery with formulations was modeled using a quasibinomial model, which accounted for the influence of each osmolyte and the interactions between osmolytes. The concentration level of sugars was modeled as a categorical variable in order to allow the possibility of a nonmonotonic relationship, as



observed experimentally. One basic assumption behind the model was that an individual cell could be described as a binary outcome, either alive or dead. With that assumption, a logistic model could be used to fit the experimental data.

$$\text{logit}(p) = \ln\left(\frac{p}{1-p}\right) = a_0 + a_1x_S + a_2x_{SA} + a_3x_{AA} + a_4x_Sx_{SA} + a_5x_Sx_{AA} + a_6x_{SA}x_{AA} \quad (2)$$

where  $p$  is the probability of live post-thaw,  $a_i$  are the regression coefficients,  $x_i$  represented the concentration levels of osmolytes and subscripts S, SA and AA stand for sugar, sugar alcohol, and amino acid, respectively. Note that  $a_1$ ,  $a_4$  and  $a_5$  depend on the concentration level of sugar. The models were fitted using the glm function from the built-in R package with a quasibinomial family. Mean plus/minus standard error was presented for all measurements. Two-tailed student  $t$ -tests were performed for two-sample comparisons to obtain  $p$ -values with a significant level set at 0.05.

## Results

### Post-thaw recovery of PBMC and Subpopulations frozen in Osmolyte Solutions

The osmolyte freezing solutions tested were developed using Jurkat cells. An initial phase of the investigation involved comparing the freezing response of PBMCs and Jurkat cells. The post-thaw recovery of PBMCs and Jurkat cells using different formulations of SGI and TGI is shown in Figure 3(a) and (b). Test formulations were generated spanning the parameter space and included the optimum formulation. The post-thaw recovery for PBMCs and Jurkat cells were comparable for optimized solution formulations; however, Jurkat cells respond poorly to sub-optimal cryoprotectants, while PBMC recovery remains high (>60%) throughout the parameter space.

### Comparisons between T-cell subpopulations

The next phase of the investigation involved characterizing the post-thaw recovery of T-cell subsets cryopreserved in candidate DMSO-free solutions. Subpopulations of T-cells are used therapeutically and as a result, a comparison of post-thaw recovery for T-cell subpopulations is of interest. In Figure 4(a) the distribution of cell types found in the PBMCs products is given. Lymphocytes (CD14-CD15-) were a major subset (84%), followed by monocytes (CD14+, 14%) and granulocytes (CD15+, 2%). Of the lymphocyte population, Helper T (CD3+CD4+, 41%) was the major subset, followed by B (CD19+, 16%) Cytotoxic T (CD3+CD8+, 14%), NK (CD3-CD56+10%) and NK T (CD3+CD56+, 3%). The standard error of each population was less than 5%.

The comparison of post-thaw recoveries for Jurkat cells, all CD3+ T-cells, and helper T-cell and cytotoxic T-cell subsets for three high-performing cryoprotectants (SGI, TGI, MGI) is shown in Figure 4(b). The post-thaw recovery of primary T-cells (CD3+ cells) and helper T-cells was higher than Jurkat cells for all cryoprotectants, while cytotoxic T-cells had the lowest post-thaw recovery. DMSO-free cryoprotectants showed higher post-thaw recoveries of human helper T-cell (CD3+CD4+) compared to Jurkat cells ( $p < 0.05$ ). DMSO-free cryoprotectants showed lower post-thaw recoveries for cytotoxic T-cells (CD3+CD8+)

compared to Jurkat cells, but the DMSO-containing solution showed equivalent ( $p>0.05$ ) post-thaw recoveries between human cytotoxic T-cells (CD3+CD8+) and Jurkat cells. Figure 4(c) shows the same post-thaw recovery data as part (b), but recoveries are grouped by cryoprotectant rather than by cell type. Figure 4(c) shows that the cell types have similar recovery in DMSO (approximately 80%), but there is greater variation in their responses to DMSO-free cryoprotectants.

There was no significant difference between all three DMSO-free cryoprotectants for primary human T-cells. For human helper T-cells, there was no significant difference between the three DMSO-free cryoprotectants, but there was a significant difference between TGI and DMSO ( $p=0.0225$ ) as well as SGI and DMSO ( $p=0.0418$ ). There was no significant difference between MGI and DMSO. For human cytotoxic T-cells, there was no significant difference between all four cryoprotectants. In other words, all cryoprotectants were equivalent in terms of CD8+ post-thaw recoveries. In comparison between post-thaw recoveries of CD4+ and CD8+, there were significant differences for TGI ( $p=0.0012$ ), SGI ( $p=0.0005$ ) and MGI ( $p=0.0039$ ) and no significant difference for DMSO. The differences in post-thaw recoveries between helper T-cell (CD3+CD4+) and cytotoxic T-cells (CD3+CD8+) in DMSO-free cryoprotectants indicated the necessity to optimize the formulations in order to improve post-thaw recoveries of both groups as high as possible and as equivalent as possible.

### Optimization of DMSO-free cryoprotectant to cryopreserve dual subsets of T-cells

TGI was selected to be optimized with the differential evolution algorithm due to higher post-thaw recoveries in the average of T-cell (CD3+), helper T-cell (CD3+CD4+) and cytotoxic T-cell (CD3+CD8+) among all three DMSO-free cryoprotectants (Figure 4(c)). A variant of the DE algorithm, differential evolution of multi-objective (DEMO), was used to identify the optimal formulations with the highest post-thaw recoveries of helper T-cell (CD3+CD4+) and cytotoxic T-cell (CD3+CD8+) generation by generation, as shown in Figure 5(a) and 5(b), respectively. Generations 0, 1 and 2 showed significant variations of post-thaw recoveries of both CD4+ and CD8+ for the different compositions tested, but by generation, the differences in post-thaw viability between the different compositions tested had been reduced to below 20%. The evolutionary optimization showed the improvement of two subsets simultaneously as shown in Figure 5(c) from divergence to convergence as well as from low to high post-thaw recovery. The post-thaw recoveries of helper T-cells were generally proportional to but higher than cytotoxic T-cell recovery. The maximum post-thaw recoveries of helper and cytotoxic were 103% and 73%, respectively.

The optimization of two subsets of CD3+ T-cells might deoptimize another subset of CD3+ T-cells present in the sample. For example, two TGI formulations exhibited over 80% post-thaw recoveries of NK T-cell (CD3+CD56+) in generation 1, but these two formulations were excluded in generation 3 because they resulted in relatively lower post-thaw recoveries of helper T-cells and cytotoxic T-cells, as shown in Figure 5(d). In addition, the average post-thaw recovery of generation 1 was greater in generation 1 (56%) than generation 2 (33%) but had rebounded by generation 3 (58%).



## Statistical modeling of freezing response between PBMC subsets

Statistical models can be used to characterize the role and interactions between different osmolytes in the TGI cryoprotectant across different PBMC subsets [20,21]. The statistical models indicated the difference between helper T-cells (CD3+CD4+) and cytotoxic T-cells (CD3+CD8+) (see supplement). For helper T-cells, the level 1 trehalose and its interaction with glycerol and isoleucine dominated the post-thaw recovery and high-level trehalose resulted in negative effects. This trend was similar to Jurkat cells as seen in our previous work [20,21]. For cytotoxic T-cells, however, a specific level of trehalose was preferred, and there were weak interactions between trehalose and glycerol and trehalose and isoleucine.

The corresponding statistical model for NK T-cells was also established. The statistical model suggested low-level trehalose was dominant but the interaction of low-level trehalose and glycerol was not beneficial for NK T-cells. Prediction versus truth plots matching models to actual post-thaw recovery showed all predicted points had over 80% accuracy for both helper T-cells and cytotoxic T-cells as shown in Figure 6(a) and 6(b), respectively. Figure 6(c) shows that the statistical model underestimated several individuals in the prediction of the post-thaw recovery of NK T-cells.

## Post-thaw culture

Samples of PBMCs that were cryopreserved with either DMSO or TGI (chosen as a representative DMSO-free cryoprotectant) were cultured for 72 hours post-thaw to determine post-thaw cell losses. Cells were not stimulated with cytokines, so proliferation did not occur. Both populations of PBMCs diminished 24 hours post-thaw but stabilized over the next two days (Figure 7(a)), with TGI frozen cells performing over 0.1 million cells more than DMSO 24 hours post-thaw. Similarly, TGI frozen cells showed over 10% higher viability than DMSO (Figure 7(b)) over the same time frame.

## Stability of samples post thaw

Samples of PBMCs cryopreserved in TGI (representative DMSO-free cryoprotectant) were stained for surface markers, viability and caspases (apoptosis) immediately post-thaw and 24 hours post-thaw. Samples were stained with antibodies for CD4 and CD8 T-cells to determine how these T-cell types respond to preservation in DMSO-free cryoprotectants. Immediately post-thaw, 72% of CD4+ T-cells were alive (34% no apoptosis, 37% in early apoptosis), and 67% of CD8+ T-cells were alive (22% no apoptosis, 45% in early apoptosis). After 24 hours, the total number of live cells for CD4+ and CD8+ cells had dropped (55% and 57%, respectively), but fewer live cells showed markers for apoptosis. Table 3 shows the viability of CD4+ and CD8+ cells 0 and 24 hours post-thaw, while Table 4 further identifies viable and dead cells as live (7-AAD- FLICA-), early apoptosis (7-AAD- FLICA+), late apoptosis (7-AAD+ FLICA+), and necrosis (7-AAD+ FLICA-).

## Differential Scanning Calorimetry (DSC)

The thermophysical properties of both DMSO-free and DMSO-containing cryoprotectant solutions including melting temperature, enthalpy of melting, glass transition temperature ( $T_g$ ) and softening temperature ( $T_s$ ) were measured via DSC as listed in Table 5. TGI was found to have the lowest melting temperature and lowest enthalpy of melting. In contrast,

DMSO had the highest melting temperature as well as enthalpy of melting, and the lowest glass transition temperature. There was no significant difference between DMSO-free cryoprotectants in terms of  $T_g$  and  $T_s$ .

## Discussion and Conclusion

There has been great interest in finding nontoxic alternatives to DMSO that can cryopreserve cells effectively. Previous work has shown the potential of combining osmolytes (sugars, glycerol and amino acids) as DMSO-free cryoprotectants were effective for cryopreserving Jurkat cells with high post-thaw recovery [20,21,24]. This work expands this approach for the preservation of primary human PBMCs as well as specific subsets contained therein.

DMSO-free cryoprotectants showed competitive post-thaw recovery of PBMCs (CD45+) compared to DMSO-containing solutions, and higher preservation capability for primary T-cells and helper T-cells. Cytotoxic T-cells showed low post-thaw recovery for DMSO-free solutions compared to helper T-cells, indicating that DMSO-free cryoprotectants composed of osmolytes may not be sufficient to preserve all immune cells. These cell types may require other compounds to enhance preservation quality, such as IL-2, human serum albumin (HSA) and other cytokines or metabolic factors. In addition, some subsets, such as cytotoxic T-cells, might be separated and cryopreserved individually in order to eliminate regulatory signaling from other cell types.

Long-term post-thaw stability is an important consideration for the cryopreservation of PBMCs. PBMCs frozen in TGI showed higher post-thaw viability and cell concentration compared to cells frozen in DMSO over the course of 72 hours. Cells frozen in both TGI and DMSO showed a drop in viability and cell concentration 24 hours post thaw, which is likely due to cells undergoing apoptosis. Apoptosis has long been considered a contributing factor in poor cryopreservation outcomes of lymphocytes [31–34]. Recent studies of the cryopreservation of CAR-T-cells found up-regulation in apoptotic markers for CAR-T-cells frozen in DMSO compared to fresh cells [6,35]. An apoptosis assay for PBMCs frozen in TGI showed a decrease in cell viability after 24 hours in culture for both CD4+ and CD8+ T-cells. However, for both cell types immediately post-thaw, a high number of viable cells showed markers for early apoptosis. After 24 hours, although the total number of viable T-cells decreased, the percentage of healthy cells with no caspase activation (not in early apoptosis) had increased for both populations. Overall, the post-thaw stability of PBMCs showed DMSO-free cryoprotectants had higher survival rates long term after thawing, which indicated DMSO-free cryoprotectants may accelerate the enrichment process in manufacturing cellular therapy products. The apoptosis assay revealed that helper T-cells and cytotoxic T-cells are prone to apoptosis immediately post-thaw. Apoptosis inhibitors could be incorporated into the DMSO-free cryoprotectants to reduce apoptosis in the first 24 hours after thawing.

The formulations of DMSO-free cryoprotectants were optimized using a differential evolution algorithm for multiple objectives (DEMO) and localized several compatible formulations including the original formulations. The results of the DEMO algorithm confirmed our previous work [20–22,24], which started from an immortalized CD3+ T-cell

line and found one optimal formulation for each group of osmolytes. These formulations of DMSO-free cryoprotectants presented similar post-thaw recoveries for human T-cells and the Jurkat cell line, as well as higher post-thaw recovery of helper T-cells, compared to DMSO. These results not only confirm that osmolyte mixtures can serve as an effective alternative to DMSO with human primary cells, but also show that the methodology we previously developed for immortalized cell lines can be directly applied to primary cells.

Conventional wisdom indicates that successful cryopreservation involves the control of ice formation during freezing [36]. In this study, we determined the thermophysical properties of each cryoprotectant solution and found that TGI had the lowest enthalpy of melting, indicating less ice formation. However, TGI was not the optimal cryoprotectant for every cell type, indicating that the amount of ice formed during freezing is not the only contributing factor to cell recovery. This study showed distinct differences in cell recovery for helper T-cells and cytotoxic T-cells. Helper T-cells showed higher cell recovery across all the cryoprotectant compositions tested. Helper T-cells and cytotoxic T-cells were optimized together: cryoprotectants that increased helper T-cell recovery also increased cytotoxic T-cell recovery. NKT cells, another T-cell subset, did not optimize simultaneously with the other two subsets. NK cells, although not included in this study, are known to suffer from poor cryopreservation outcomes [37–39]. These cell types (cytotoxic T-cells, NKT cells, and NK cells), which share similar cytotoxic functions, also share a sensitivity to cryopreservation that is not seen with helper T-cells [40–42]. These results suggest that biology is a contributing factor to cryopreservation. Improving the recovery of cell types that are especially sensitive to cryopreservation will depend not only on the interactions between cryoprotectants and water, but also on the biological interactions between cryoprotectants and cells.

The DMSO-free cryoprotectants can be used to achieve high post-thaw recovery of many subpopulations of PBMCs but developing customized cryoprotectants will likely still be necessary to optimize recovery of all of the subsets of interest. The optimization of dual subsets might result in bias to another subset, which indicates the difficulty of cryopreserving all subsets in a heterogeneous population with a universal solution. However, this phenomenon indicates that cryopreservation could become an alternative label-free method to automatically sort out targeted subsets. In other words, undesired subsets can be naturally removed in cryopreservation with specific formulations to avoid the process of cell sorting.

In this study, we expanded upon our previous cryopreservation of Jurkat cells to demonstrate the potential for DMSO-free preservation of multiple cell types in PBMCs. It is clear that these cell types have different responses to cryoprotectants, and there may not be a universal cryoprotectant that can optimize all subsets simultaneously. Ultimately, understanding the freezing responses of different subsets of PBMCs will allow for more effective cryopreservation of PBMCs based on their intended downstream application.

## Supplementary Material

Refer to Web version on PubMed Central for supplementary material.

## Acknowledgments

This work was funded by the National Institutes of Health under R01EB023880. The authors would like to thank Prof. Keli Hippen, Sangya Subgh and Sophia Shani for their help in the preliminary stage. The authors would also like to thank the Translational Therapy Lab for performing phenotype characterization with flow cytometry in the University of Minnesota.

## Reference

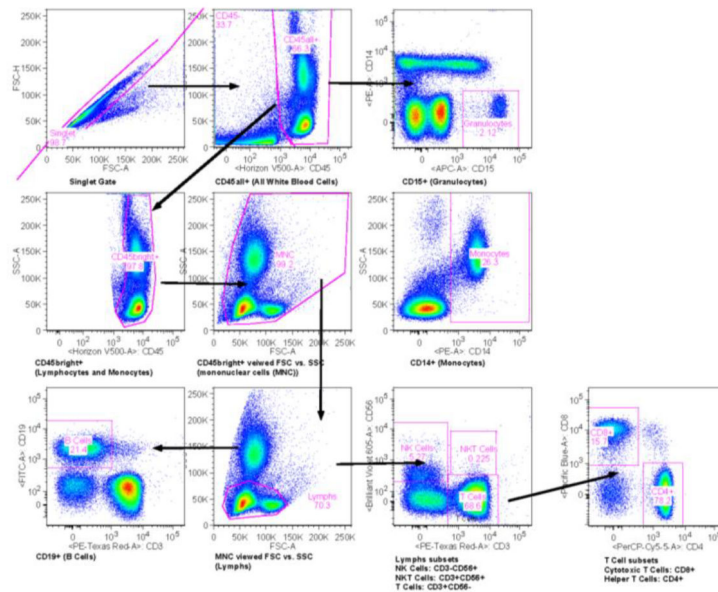
- [1]. Institute TNC. CAR T Cells: Engineering Patients' Immune Cells to Treat Their Cancers 2017.
- [2]. Pettitt D, Arshad Z, Smith J, Stanic T, Holländer G, Brindley D. CAR-T Cells: A Systematic Review and Mixed Methods Analysis of the Clinical Trial Landscape. *Mol Ther* 2018;26:342–53. doi:10.1016/j.ymthe.2017.10.019. [PubMed: 29248427]
- [3]. Lovelock JE, Bishop MWH. Prevention of Freezing Damage to Living Cells by Dimethyl Sulphoxide. *Nature* 1959;183:1394–5. doi:10.1038/1831394a0. [PubMed: 13657132]
- [4]. Liang X, Hu X, Hu Y, Zeng W, Zeng G, Ren Y, et al. Recovery and functionality of cryopreserved peripheral blood mononuclear cells using five different xeno-free cryoprotective solutions. *Cryobiology* 2019;86:25–32. doi:10.1016/j.cryobiol.2019.01.004. [PubMed: 30629948]
- [5]. Baboo J, Kilbride P, Delahaye M, Milne S, Fonseca F, Blanco M, et al. The Impact of Varying Cooling and Thawing Rates on the Quality of Cryopreserved Human Peripheral Blood T Cells. *Sci Rep* 2019;9:3417. doi:10.1038/s41598-019-39957-x. [PubMed: 30833714]
- [6]. Xu H, Cao W, Huang L, Xiao M, Cao Y, Zhao L, et al. Effects of cryopreservation on chimeric antigen receptor T cell functions. *Cryobiology* 2018;83:40–7. doi:10.1016/j.cryobiol.2018.06.007. [PubMed: 29908946]
- [7]. de Abreu Costa L, Henrique Fernandes Ottoni M, dos Santos M, Meireles A, Gomes de Almeida V, de Fátima Pereira W, et al. Dimethyl Sulfoxide (DMSO) Decreases Cell Proliferation and TNF- $\alpha$ , IFN- $\gamma$ , and IL-2 Cytokines Production in Cultures of Peripheral Blood Lymphocytes. *Molecules* 2017;22:1789. doi:10.3390/molecules22111789.
- [8]. Luo Y, Wang P, Liu H, Zhu Z, Li C, Gao Y. The state of T cells before cryopreservation: Effects on post-thaw proliferation and function. *Cryobiology* 2017;79:65–70. doi:10.1016/j.cryobiol.2017.08.008. [PubMed: 28863950]
- [9]. Germann A, Oh Y-J, Schmidt T, Schön U, Zimmermann H, von Briesen H. Temperature fluctuations during deep temperature cryopreservation reduce PBMC recovery, viability and T-cell function. *Cryobiology* 2013;67:193–200. doi:10.1016/j.cryobiol.2013.06.012. [PubMed: 23850825]
- [10]. Nazarpour R, Zabihi E, Alijanpour E, Abedian Z, Mehdizadeh H, Rahimi F. Optimization of Human Peripheral Blood Mononuclear Cells (PBMCs) Cryopreservation. *Int J Mol Cell Med* 2012;1:88–93. [PubMed: 24551763]
- [11]. Fahy GM. The relevance of cryoprotectant “toxicity” to cryobiology. *Cryobiology* 1986;23:1–13. doi:10.1016/0011-2240(86)90013-1. [PubMed: 3956226]
- [12]. Mallone R, Mannering SI, Brooks-Worrell BM, Durinovic-Belló I, Cilio CM, Wong FS, et al. Isolation and preservation of peripheral blood mononuclear cells for analysis of islet antigen-reactive T cell responses: position statement of the T-Cell Workshop Committee of the Immunology of Diabetes Society. *Clin Exp Immunol* 2011;163:33–49. doi:10.1111/j.1365-2249.2010.04272.x. [PubMed: 20939860]
- [13]. Best A, Hidalgo G, Mitchell K, Yannelli JR. Issues concerning the large scale cryopreservation of peripheral blood mononuclear cells (PBMC) for immunotherapy trials. *Cryobiology* 2007;54:294–7. doi:10.1016/j.cryobiol.2007.02.002. [PubMed: 17433284]
- [14]. Angel S, von Briesen H, Oh Y-J, Baller MK, Zimmermann H, Germann A. Toward Optimal Cryopreservation and Storage for Achievement of High Cell Recovery and Maintenance of Cell Viability and T Cell Functionality. *Biopreserv Biobank* 2016;14:539–47. doi:10.1089/bio.2016.0046. [PubMed: 27792414]
- [15]. Jeurink PV, Vissers YM, Rappard B, Savelkoul HFJ. T cell responses in fresh and cryopreserved peripheral blood mononuclear cells: Kinetics of cell viability, cellular subsets, proliferation, and

- cytokine production. *Cryobiology* 2008;57:91–103. doi:10.1016/j.cryobiol.2008.06.002. [PubMed: 18593572]
- [16]. Yang J, Diaz N, Adelsberger J, Zhou X, Stevens R, Rupert A, et al. The effects of storage temperature on PBMC gene expression. *BMC Immunol* 2016;17:6. doi:10.1186/s12865-016-0144-1. [PubMed: 26979060]
- [17]. Hønge BL, Petersen MS, Olesen R, Møller BK, Erikstrup C. Optimizing recovery of frozen human peripheral blood mononuclear cells for flow cytometry. *PLoS One* 2017;12:e0187440. doi:10.1371/journal.pone.0187440. [PubMed: 29091947]
- [18]. Kety Pratt Riccio E, Neves I, Maria Banic D, Corte-Real S, das Graças Alecrim M, Morgado M, et al. Cryopreservation of peripheral blood mononuclear cells does not significantly affect the levels of spontaneous apoptosis after 24-h culture. *Cryobiology* 2002;45:127–34. doi:10.1016/S0011-2240(02)00121-9. [PubMed: 12482378]
- [19]. Mathur A, Tripathi A, Kuse M. Scalable system for classification of white blood cells from Leishman stained blood stain images. *J Pathol Inform* 2013;4:15. doi:10.4103/2153-3539.109883. [PubMed: 23858390]
- [20]. Pi C-H, Yu G, Dosa PI, Hubel A. Characterizing modes of action and interaction for multicomponent osmolyte solutions on Jurkat cells. *Biotechnol Bioeng* 2019;116:631–43. doi:10.1002/bit.26880. [PubMed: 30475391]
- [21]. Pi C-H, Yu G, Petersen A, Hubel A. Characterizing the “sweet spot” for the preservation of a T-cell line using osmolytes. *Sci Rep* 2018;8:16223. doi:10.1038/s41598-018-34638-7. [PubMed: 30385865]
- [22]. Yu G, Yap YR, Pollock K, Hubel A. Characterizing Intracellular Ice Formation of Lymphoblasts Using Low-Temperature Raman Spectroscopy. *Biophys J* 2017;112:2653–63. doi:10.1016/j.bpj.2017.05.009. [PubMed: 28636921]
- [23]. Pollock K, Budenske JW, McKenna DH, Dosa PI, Hubel A. Algorithm-driven optimization of cryopreservation protocols for transfusion model cell types including Jurkat cells and mesenchymal stem cells. *J Tissue Eng Regen Med* 2017;11:2806–15. doi:10.1002/term.2175. [PubMed: 27229375]
- [24]. Pollock K, Yu G, Moller-Trane R, Koran M, Dosa PI, McKenna DH, et al. Combinations of Osmolytes, Including Monosaccharides, Disaccharides, and Sugar Alcohols Act in Concert During Cryopreservation to Improve Mesenchymal Stromal Cell Survival. *Tissue Eng Part C Methods* 2016;22:999–1008. doi:10.1089/ten.tec.2016.0284. [PubMed: 27758133]
- [25]. Yu G, Li R, Hubel A. Interfacial Interactions of Sucrose during Cryopreservation Detected by Raman Spectroscopy. *Langmuir* 2019;35:7388–95. doi:10.1021/acs.langmuir.8b01616. [PubMed: 30398347]
- [26]. Yancey P, Clark M, Hand S, Bowlus R, Somero G. Living with water stress: evolution of osmolyte systems. *Science* (80- ) 1982;217:1214–22. doi:10.1126/science.7112124.
- [27]. Dietz AB, Bulur PA, Emery RL, Winters JL, Epps DE, Zubair AC, et al. A novel source of viable peripheral blood mononuclear cells from leukoreduction system chambers. *Transfusion* 2006;46:2083–9. doi:10.1111/j.1537-2995.2006.01033.x. [PubMed: 17176319]
- [28]. Storn R, Price K. Differential Evolution – A Simple and Efficient Heuristic for global Optimization over Continuous Spaces. *J Glob Optim* 1997;11:341–59. doi:10.1023/A:100820282.
- [29]. Robi T, Filipi B. DEMO: Differential Evolution for Multiobjective Optimization Int. Conf. Evol. Multi-Criterion Optim, Springer, Berlin, Heidelberg; 2005, p. 520–33. doi:10.1007/978-3-540-31880-4\_36.
- [30]. Pi C-H, Dosa PI, Hubel A. Differential Evolution for the Optimization of DMSO-free Cryoprotectants: Influence of Control Parameters. *J Biomech Eng* 2019. doi:10.1115/1.4045815.
- [31]. BAUST JM, VAN BUSKIRKR, BAUST JG. CELL VIABILITY IMPROVES FOLLOWING INHIBITION OF CRYOPRESERVATION-INDUCED APOPTOSIS. *Vitr Cell Dev Biol* 2000;36:262–70. doi:10.1290/1071-2690(2000)036<0262:CVIFIO>2.3.CO;2.
- [32]. Sarkar S, Kalia V, Montelaro RC. Caspase-mediated apoptosis and cell death of rhesus macaque CD4+ T-cells due to cryopreservation of peripheral blood mononuclear cells can be rescued by

- cytokine treatment after thawing. *Cryobiology* 2003;47:44–58. doi:10.1016/S0011-2240(03)00068-3. [PubMed: 12963412]
- [33]. Stroh C, Cassens U, Samraj AK, Sibrowski W, Schulze-Osthoff K, Los M. The role of caspases in cryoinjury: caspase inhibition strongly improves the recovery of cryopreserved hematopoietic and other cells. *FASEB J* 2002;16:1651–3. doi:10.1096/fj.02-0034fje. [PubMed: 12207004]
- [34]. Chong EA, Levine BL, Grupp SA, Davis M, Siegel DL, Maude SL, et al. CD19-Directed CAR T-Cell (CTL019) Product Viability and Clinical Outcomes in Non-Hodgkin Lymphomas and B-Cell Acute Lymphoblastic Leukemia. *Blood* 2018;132:197–197. doi:10.1182/blood-2018-197. [PubMed: 29784641]
- [35]. Panch SR, Srivastava SK, Elavia N, McManus A, Liu S, Jin P, et al. Effect of Cryopreservation on Autologous Chimeric Antigen Receptor T Cell Characteristics. *Mol Ther* 2019;27:1275–85. doi:10.1016/j.ymthe.2019.05.015. [PubMed: 31178392]
- [36]. Fahy GM, Wovk B. Principles of Cryopreservation by Vitrification. *Methods Mol. Biol.* (Methods Protoc, vol. 1257, 2015, p. 21–82. doi:10.1007/978-1-4939-2193-5\_2.
- [37]. Mata MM, Mahmood F, Sowell RT, Baum LL. Effects of cryopreservation on effector cells for antibody dependent cell-mediated cytotoxicity (ADCC) and natural killer (NK) cell activity in 51Cr-release and CD107a assays. *J Immunol Methods* 2014;406:1–9. doi:10.1016/j.jim.2014.01.017. [PubMed: 24561308]
- [38]. Kashfiolasl F, Khoeiniha S, Rad PM. Cancer therapy challenges, Versus Natural killer cells 2015.
- [39]. El Assal R, Abou- Elkacem L, Tocchio A, Pasley S, Matosevic S, Kaplan DL, et al. Bioinspired Preservation of Natural Killer Cells for Cancer Immunotherapy. *Adv Sci* 2019;6:1802045. doi:10.1002/advs.201802045.
- [40]. Kerkvliet N, Lawrence BP. Cytotoxic T Cells\*. *Compr. Toxicol*, vol. 126, Elsevier; 2010, p. 109–32. doi:10.1016/B978-0-08-046884-6.00606-0.
- [41]. Yu KOA, Porcelli SA. The diverse functions of CD1d-restricted NKT cells and their potential for immunotherapy. *Immunol Lett* 2005;100:42–55. doi:10.1016/j.imlet.2005.06.010. [PubMed: 16083968]
- [42]. Fang F, Xiao W, Tian Z. NK cell-based immunotherapy for cancer. *Semin Immunol* 2017;31:37–54. doi:10.1016/j.smim.2017.07.009. [PubMed: 28838796]



(a)



(b)

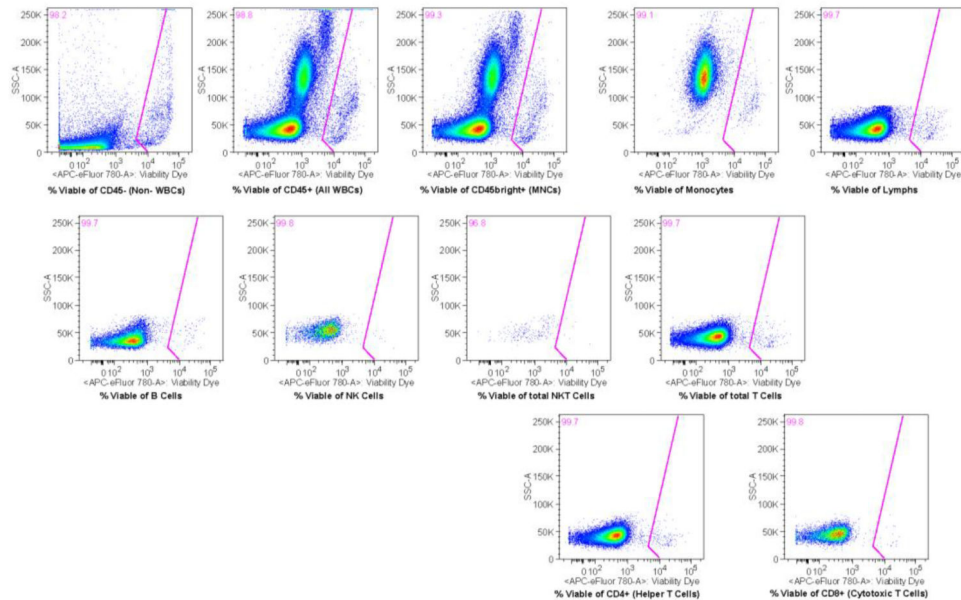


**Figure 1.**

Gating strategy to identify proportions of PBMC (a) subsets and (b) viabilities through flow cytometry. A total of 30000 singlet events was collected (top left plot). First, white blood cell (CD45+) was identified from singlets. Granulocytes (CD15+), monocytes (CD14+) and lymphocytes (CD14-CD15-) were identified from white blood cell (CD45+). B cell (CD19+), natural killer cell (CD3-CD56+), natural killer T-cell (CD3+CD56+) and T-cell (CD3+CD56-) were identified from lymphocytes. Helper T-cell (CD3+CD4+) and cytotoxic T-cell (CD3+CD8+) were identified from T-cells.

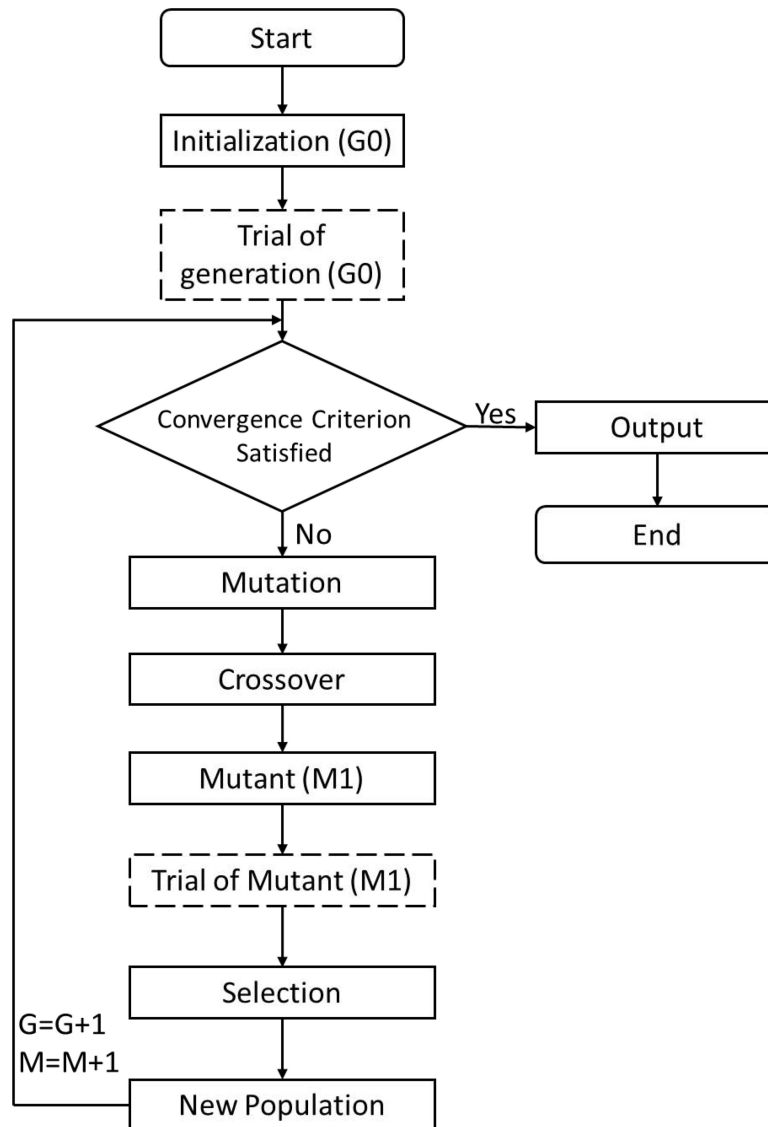


**Figure 2.**

The Differential Evolution algorithm flow chart, with steps noted with straight lines representing algorithm steps and steps denoted with dashed lines representing experimental steps. The initial population of generation (G0) is randomly generated and spans the parameter space. A trial population (M1) is based on the mutation of G0. The post-thaw recovery of G0 vector and the M1 vectors are measured experimentally, producing an emergent population, which is further mutated in subsequent generations.

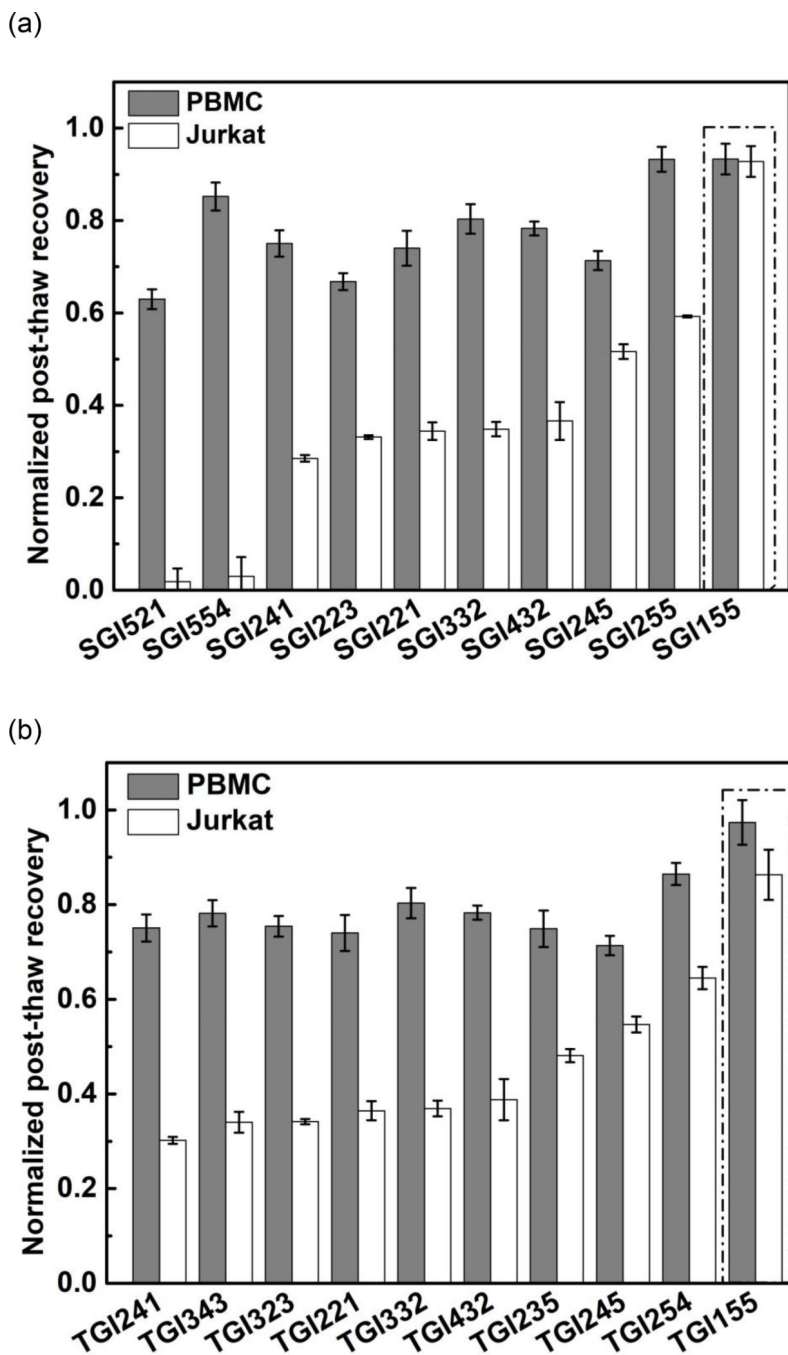


**Figure 3.** Comparison of normalized post-thaw recoveries between Jurkat and PBMC (CD45+) based on the DE algorithm for cryoprotectants (a) SGI and (b) TGI. The post-thaw recoveries were normalized to a 10% DMSO control. SGI155 and TGI155 were the optimal formulations (boxed).

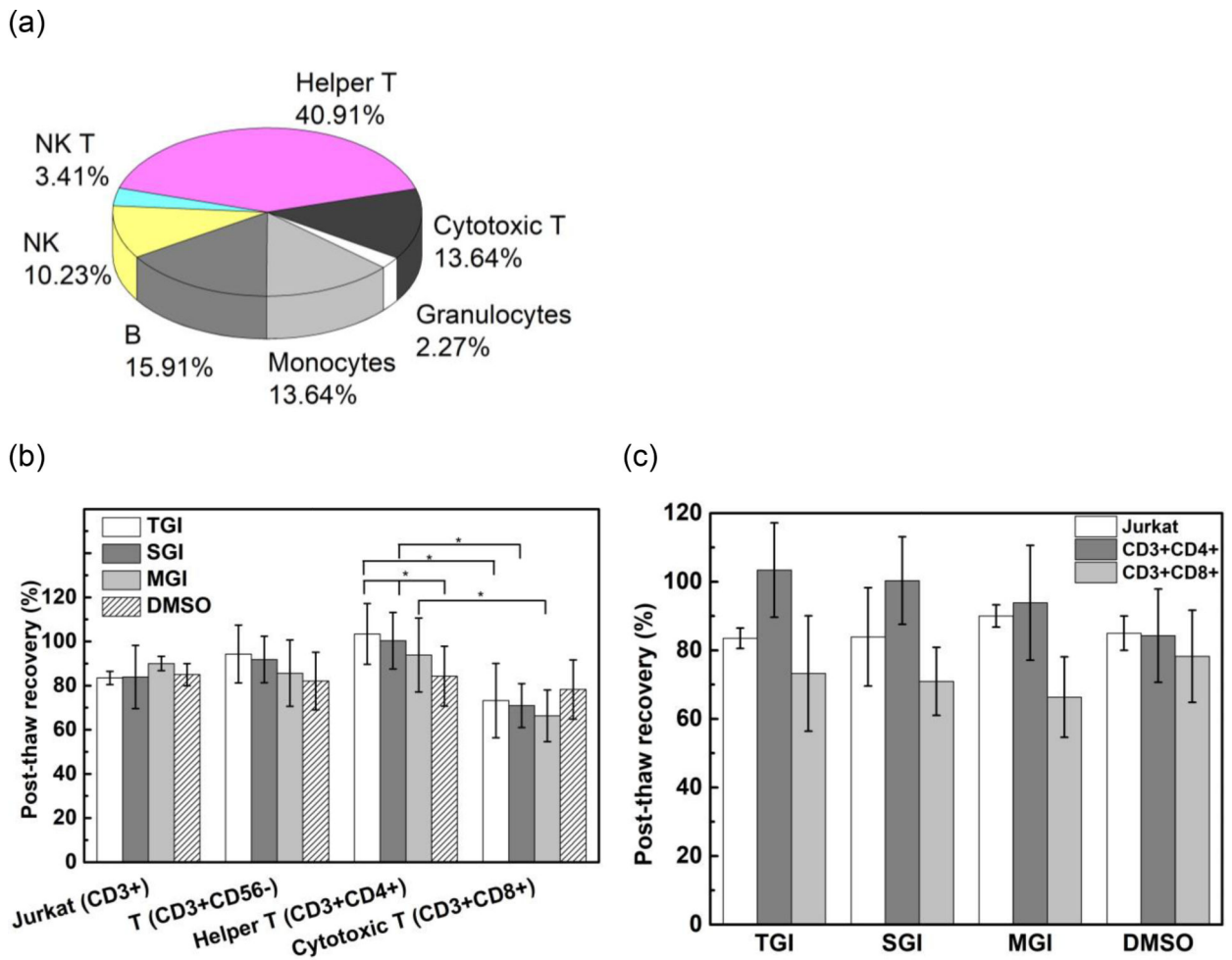


**Figure 4.**

(a) The average proportions of major populations present in PBMC samples (left) and the proportions of lymphocyte subpopulations (n=10). (b) The post-thaw recoveries of Jurkat cells and lymphocyte subpopulations with three DMSO-free and one DMSO-containing cryoprotectants under cooling rate 1°C/min (n=10). (c) The post-thaw recoveries from part (b) grouped by cryoprotectant.

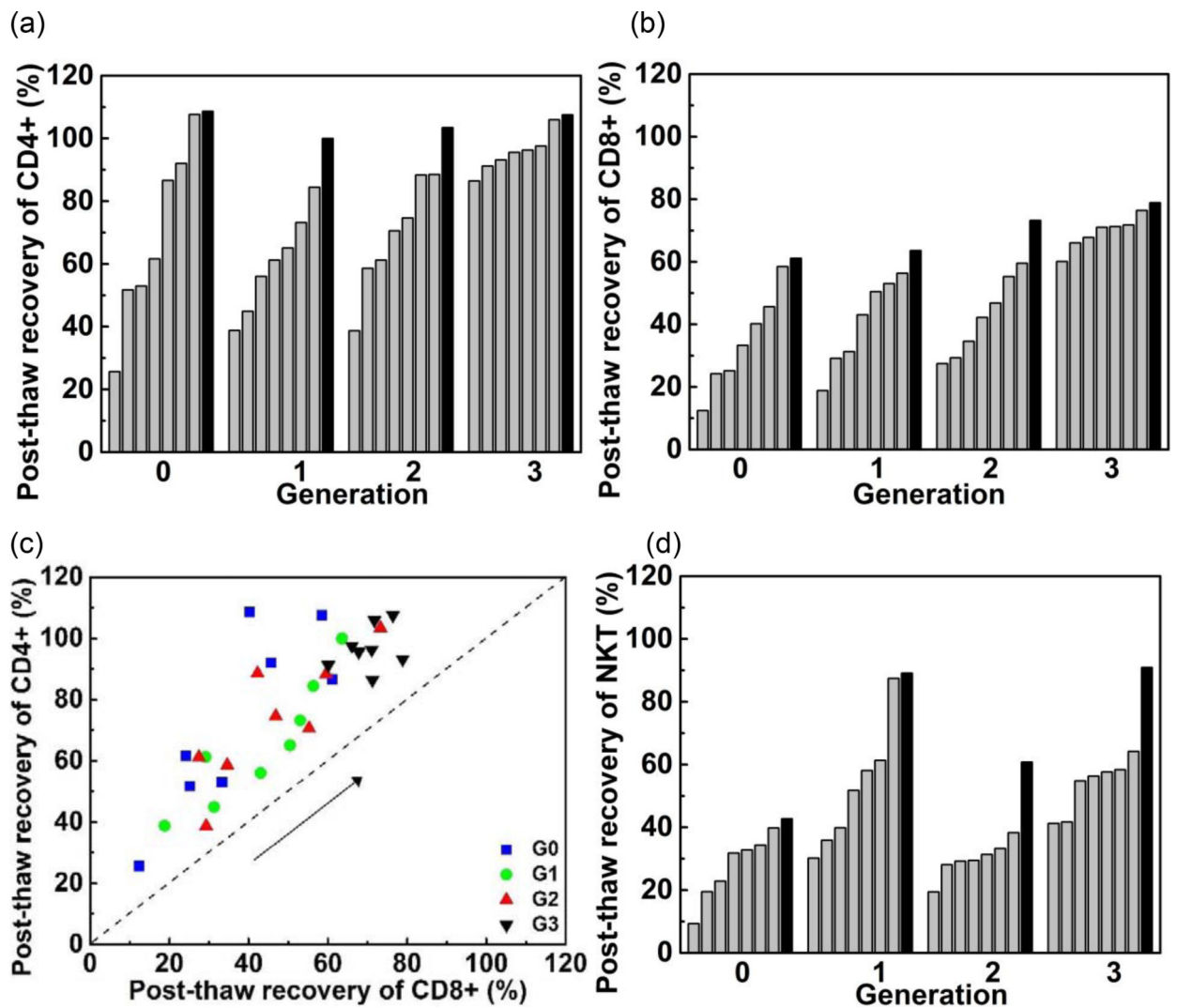


**Figure 5.**

TGI formulations were optimized using the differential evolution for multi-objective (DEMO) algorithm to maximize helper T-cell and cytotoxic t-cell recovery. Best performing solution compositions for each generation are shown in black (a) Post-thaw recoveries of helper T-cell (CD3+CD4+) using TGI formulations from Generation 0 to Generation 3. (b) Post-thaw recoveries of cytotoxic (CD3+CD8+) T-cells using TGI formulations from Generation 0 to Generation 3. (c) Post-thaw recoveries of CD4+ and CD8+ to TGI formulations generated via DEMO from Generation 0 to Generation 3. (d) Post-thaw recoveries of NKT (CD3+CD56+) cells in TGI formulations from Generation 0 to Generation 3.

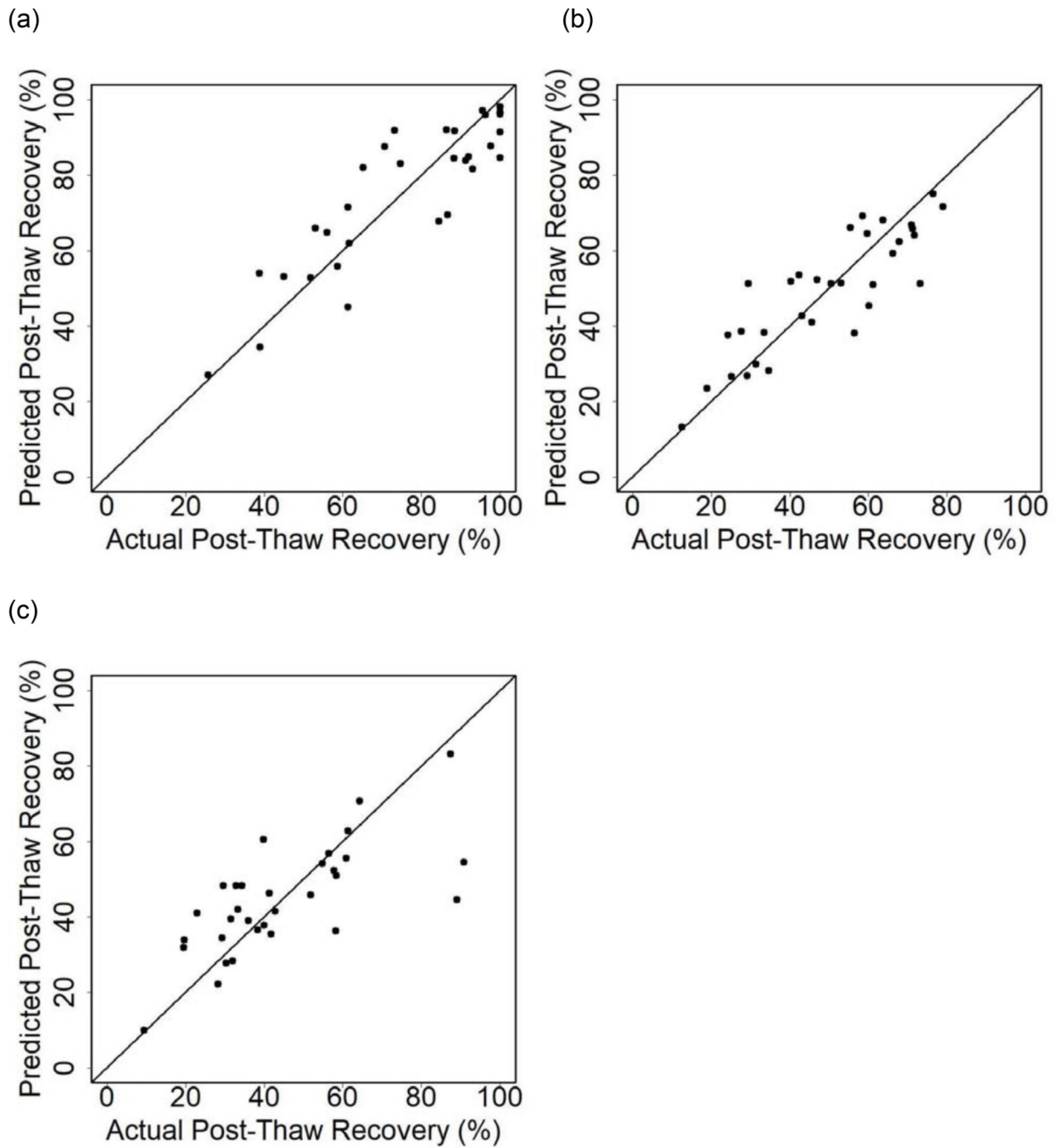


**Figure 6.**

The predicted versus actual of post-thaw recoveries using statistical models for (a) helper T-cell (CD3+CD4+), (b) cytotoxic (CD3+CD8+) and (c) NK T-cell (CD3+CD56+). The diagonal line indicates where predicted values equal actual values. (N=32)



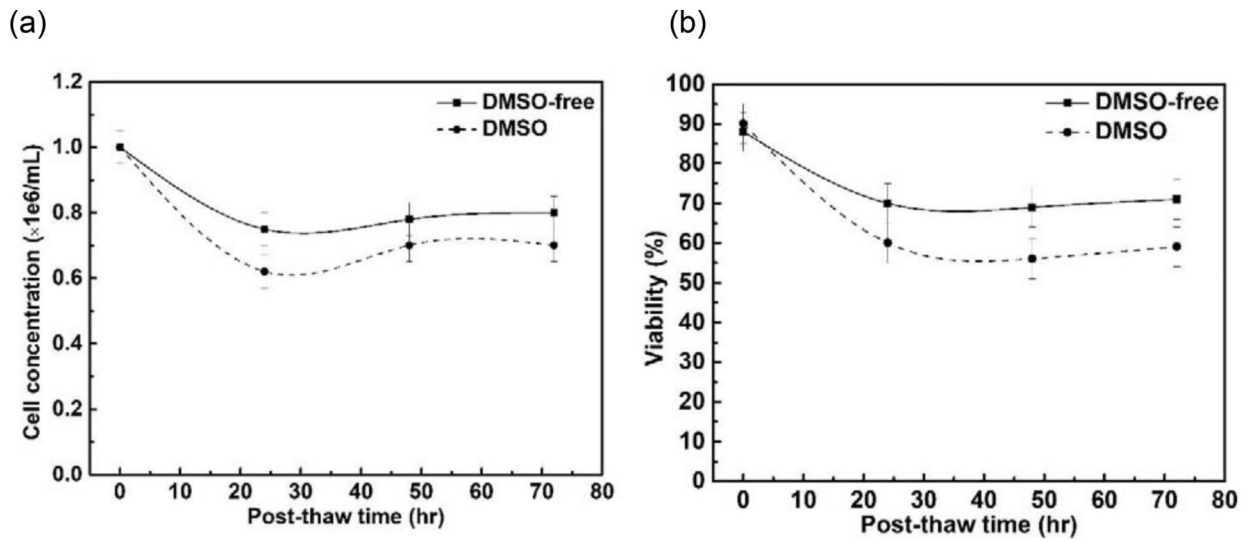


**Figure 7.** Post-thaw culture of PBMCs cryopreserved with DMSO-free and DMSO-containing cryoprotectants for 72 hours. (a) cellular concentrations and (b) cell viability. (n=9)

**Table 1.**

Information of antibodies and fluorophores of phenotype characterization

<b>Fluorophore</b>	<b>Antibody</b>	<b>Manufacturer</b>
V500	CD45	BD Horizon
PE-TR	CD3	Invitrogen
PerCP-Cy5.5	CD4	Biologend
Pacific blue	CD8	Invitrogen
BV605	CD56	Biologend
PE	CD14	BD Pharmingen
APC	CD15	BD Pharmingen
FITC	CD19	BD Biosciences
APC-ef870	Viability	Invitrogen

Author Manuscript

Author Manuscript

Author Manuscript

Author Manuscript

**Table 2.**

Antibody Information for Apoptosis Staining Protocol

<b>Fluorophore</b>	<b>Antibody</b>	<b>Manufacturer</b>
PE	CD4	Biolegend
Brilliant Violet 421	CD8	Biolegend
7-AAD	N/A	BD
FAM-FLICA	FMK	ThermoFisher

Author Manuscript

Author Manuscript

Author Manuscript

Author Manuscript

**Table 3.**

Percentage of viable CD4+ and CD8+ T-cells as a function of time post-thaw for 0 and 24 hours

Sample	CD4		CD8	
	Live	Dead	Live	Dead
0 hr	72 ± 2	28 ± 2	68 ± 4	32 ± 4
24 hr	55 ± 14	45 ± 14	58 ± 3	43 ± 3

Author Manuscript

Author Manuscript

Author Manuscript

Author Manuscript

**Table 4.**

Percentage of CD4+ and CD8+ T-cells that are apoptotic or necrotic as a function of time post-thaw for 0 and 24 hours

Sample	CD4				CD8			
	Live	Early Apoptosis	Late Apoptosis	Necrosis	Live	Early Apoptosis	Late Apoptosis	Necrosis
0 hr	34 ± 5	38 ± 6	26 ± 1	2 ± 1	22 ± 3	46 ± 6	30 ± 3	2 ± 2
24 hr	49 ± 21	7 ± 8	43 ± 15	2 ± 2	40 ± 15	18 ± 14	42 ± 3	0 ± 1

Author Manuscript

Author Manuscript

Author Manuscript

Author Manuscript

**Table 5.**

The thermophysical properties of both DMSO and DMSO-free cryoprotectants

	<b>Melting Temperature (°C)</b>	<b>Enthalpy of Melting (J/g)</b>	<b>T<sub>g</sub> (°C)</b>	<b>T<sub>s</sub> (°C)</b>
DMSO	-9.63	195.7	-120.77	-
SGL	-11.58	191.5	-93.90	-65.08
TGI	-13.35	132.6	-94.55	-64.90
MGI	-12.43	184.9	-93.76	-65.94
LGI	-11.99	190.4	-95.42	-67.10